Journal of Photochemistry and Photobiology A: Chemistry 200 (2008) 432–437

Contents lists available at ScienceDirect

Journal of Photochemistry and Photobiology A: Chemistry

journal homepage: www.elsevier.com/locate/jphotochem

Rhodamine-conjugated acrylamide polymers exhibiting selective fluorescence enhancement at specific temperature ranges

Yasuhiro Shiraishi*, Ryo Miyamoto, Takayuki Hirai

Research Center for Solar Energy Chemistry, and Division of Chemical Engineering, Graduate School of Engineering Science, Osaka University, Toyonaka 560-8531, Japan

ARTICLE INFO

Article history:
Received 17 May 2008
Received in revised form 18 July 2008
Accepted 6 August 2008
Available online 21 September 2008

Keywords:
Acrylamide polymers
Rhodamine
Fluorescence
Temperature sensor

ABSTRACT

A simple copolymer, poly(NIPAM-*co*-RD), consisting of *N*-isopropylacrylamide (NIPAM) and rhodamine (RD) units, behaves as a fluorescent temperature sensor exhibiting selective fluorescence enhancement at a specific temperature range (25–40 °C) in water. This is driven by a heat-induced phase transition of the polymer from *coil* to *globule*. At low temperature, the polymer exists as a polar coil state and shows very weak fluorescence. At >25 °C, the polymer weakly aggregates and forms a less polar domain within the polymer, leading to fluorescence enhancement. However, at >33 °C, strong polymer aggregation leads to a formation of huge polymer particles, which suppresses the incident light absorption by the RD units and shows very weak fluorescence. In the present work, effects of polymer concentration and type of acrylamide unit in the polymer have been investigated. The increase in the polymer concentration in water leads to a formation of less polar domain even at low temperature and, hence, widens the detectable temperature range to lower temperature. Addition of *N*-*n*-propylacrylamide (NNPAM) or *N*-isopropylmethacrylamide (NIPMAM) component to the polymer, which has lower or higher phase transition temperature than that of NIPAM, enables the aggregation temperature of the polymer to shift. This then shifts the detectable temperature region to lower or higher temperature.

1. Introduction

The design and development of supramolecular systems performing as a fluorescent chemosensor have attracted a great deal of attention, since they allow rapid detection of analytes by simple fluorescence measurements [1]. Recently, fluorescent temperature sensors have attracted much attention [2–5]. So far, various kinds of fluorescent temperature sensors have been proposed; however, these exhibit monotonous emission enhancement [2,3] or quenching [4] with a rise in temperature. Earlier, we reported for the first time a fluorescent temperature sensor exhibiting selective emission enhancement at a specific temperature range in water [5]. This is based on a simple-structured copolymer, poly(NIPAM-*co*-RD) (**P1**), consisting of a thermoresponsive *N*-isopropylacrylamide (NIPAM) unit and a fluorescent rhodamine (RD) unit. The selective fluorescence enhancement is driven by a heat-induced phase transition of the polymer from *coil* to *globule*. At low temperature, the **P1** polymer exists as a polar coil state and shows very weak fluorescence. At >25 °C, the polymer aggregates to form a globule state, where a less polar domain forms within the polymer. The fluorescence quantum yield of RD increases with a decrease in the polarity of the medium [6]. Therefore, at this temperature, the polymer exhibits strong fluorescence. However, at >35 °C, the polymer strongly aggregates and forms huge polymer particles. This suppresses the incident light absorption of the RD units within the polymer and, hence, shows very weak fluorescence at >40 °C. The selective emission enhancement property of the polymer may be applicable for rough monitoring of the solution temperature, although accurate temperature detection is difficult. For example, the polymer demonstrates its ability when maintaining a solution temperature at the designated temperature range. The polymer shows strong emission at the designated temperature range; therefore, we can roughly monitor whether the solution is at the designated temperature range or not.

It is well known that temperature-induced phase transition property of the acrylamide polymers depends strongly on the polymer concentration in water [7] and the variety of acrylamide units within the polymer [3a,c–e]. In the present work, the effects of **P1** polymer concentration and the addition of other acrylamide components to the polymer on the fluorescent properties were studied. In the former part, we found that increase in the polymer concentration widens the detectable temperature range to lower temperature. In the latter part, we synthesized two more types of polymers, poly(NIPAM-*co*-NNPAM-*co*-RD) (**P2**) and

* Corresponding author. Tel.: +81 6 6850 6271; fax: +81 6 6850 6273.
E-mail address: shiraish@cheng.es.osaka-u.ac.jp (Y. Shiraishi).

1010-6030/$ – see front matter © 2008 Elsevier B.V. All rights reserved.
doi:10.1016/j.jphotochem.2008.08.020

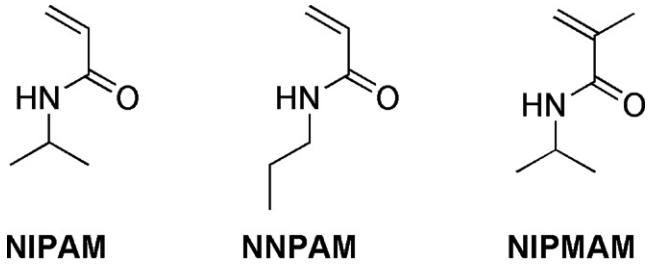

Scheme 1. Structure of respective acrylamide monomers.

poly(NIPAM-*co*-NIPMAM-*co*-RD) (**P3**), via copolymerization with *N*-*n*-propylacrylamide (NNPAM) or *N*-isopropylmethacrylamide (NIPMAM) monomer (Scheme 1), which has lower or higher phase transition temperature than that of NIPAM [3a,c–e]. We found that addition of these components to the polymer leads to a shift of the detectable temperature region to lower or higher temperature.

2. Experimental

2.1. Synthesis

All of the reagents were supplied from Wako and Tokyo Kasei. Water was purified by the Milli Q system. NIPAM and NIPMAM monomers were recrystallized from *n*-hexane prior to use, and other reagents were used without further purification. NNPAM monomer [8] and RD-conjugated diethylenetriamine (**4**) [5,9] were synthesized according to literature procedures. **P2** and **P3** polymers were synthesized in a similar manner to **P1** [5], as summarized in Scheme 2 and as follows:

2.1.1. NASI-conjugated acrylamide polymers (*P2'*, *P3'*)

NIPAM (0.34 g, 3 mmol) and NNPAM (0.34 g, 3 mmol) or NIPMAM (0.38 g, 3 mmol), *N*-hydroxysuccinimide (NASI, 20 mg, 0.12 mmol), and AIBN (15 mg, 0.089 mmol) were dissolved in *tert*-butanol (3 mL). The solution was degassed by twice freeze-pump-thaw cycles and stirred at 70 °C for 15 h under dry N_2. The resultant was concentrated by evaporation and purified by twice reprecipitation procedure with MeOH (1 mL) and diethyl ether (100 mL), affording NASI-conjugated acrylamide polymers as white solids (**P2'**, yield 87%; **P3'**, yield 77%).

2.1.2. RD-conjugated acrylamide polymers (*P2*, *P3*)

P2' or **P3'** (0.4 g) and **4** (24 mg, 0.050 mmol) were dissolved in DMF (10 mL) and stirred at room temperature for 24 h under dry N_2. The resultant was concentrated by evaporation and purified by reprecipitation procedure with MeOH (1 mL) and diethyl ether (100 mL), affording RD-conjugated acrylamide polymer, **P2** and **P3**, as light pink solids. The amount of the RD unit in the polymers was estimated by comparison of the absorbance at 341 nm with **4** in THF at 298 K [5,10]. The properties of the polymers are summarized in Table 1.

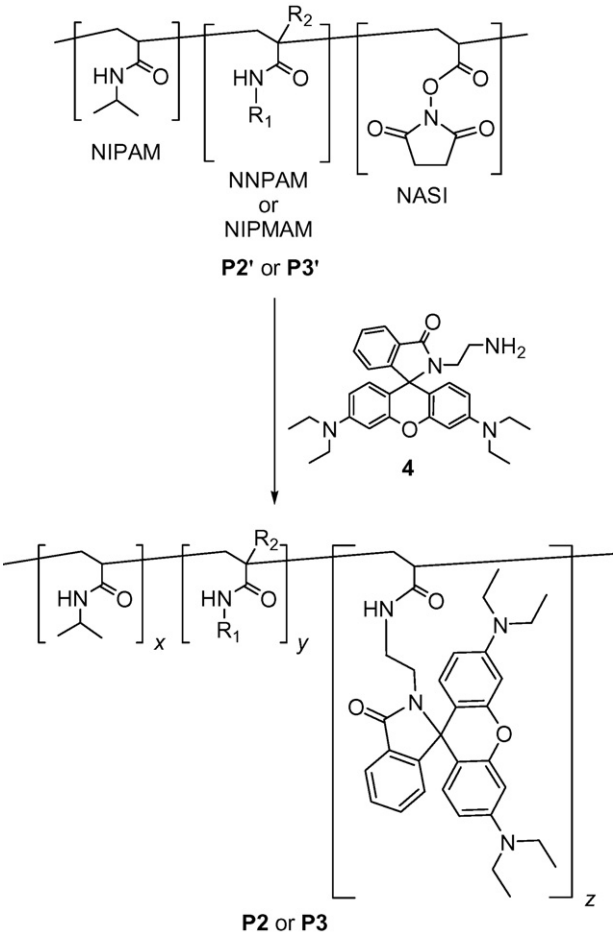

Scheme 2. Synthesis of RD-conjugated acrylamide polymers.

2.2. Measurements

Fluorescence spectra were measured on a Hitachi F-4500 fluorescence spectrophotometer (λ_{exc} = 530 nm; λ_{em} = 580 nm) with a temperature controller. Absorption spectra were measured on a UV-visible photodiode-array spectrophotometer (Shimadzu; Multispec-1500) with a temperature controller (Shimadzu; S-1700). The measurements were carried out using a 10 mm path length quartz cell [11]. After stirring the solution for 30 min at designated temperature, the measurements were carried out with continued stirring. All of the measurements were carried out in the presence of $NaClO_4$ to maintain the ionic strength of the solution (I = 0.15 M) and pH of the solution was adjusted with $HClO_4$ to 2.0 [12]. ^{1}H NMR spectra were obtained by a JEOL JNM-GSX270 Excalibur using TMS as standard. Light scattering measurements were carried out by dynamic laser scattering spectrometer (LB-500, HORIBA) (detection range, 3 nm–6 μm) and static laser scattering spectrometer (LA-910, HORIBA) (detection range 0.5–700 μm) [3i,13]. Molecular weight of the polymers was determined by GPC using a Shimadzu SCL-10A Vp system equipped with a LC-10AD

Table 1
Properties of RD-conjugated acrylamide polymers.

	Polymer	*x*/*y*/*z*	Yield (%)	M_n	M_w/M_n
P1	Poly(NIPAM$_x$-*co*-RD$_z$)	92/0/1	92	5.07×10^4	1.5
P2	Poly(NIPAM$_x$-*co*-NNPAM$_y$-*co*-RD$_z$)	74/66/1	90	2.58×10^4	1.5
P3	Poly(NIPAM$_x$-*co*-NIPMAM$_y$-*co*-RD$_z$)	63/72/1	85	4.82×10^4	2.1

Vp pump (Shimadzu) and a refractive index detector RID-10A (Shimadzu) with GPC-805 column (Shimadzu). The oven temperature was 40 °C, and THF was used as the carrier solvent (flow rate: 0.5 mL min^{-1}) [14].

3. Results and discussion

3.1. Fluorescence properties of *P1*

Fluorescence properties of poly(NIPAM-*co*-RD) (**P1**) measured with 0.2 g L^{-1} concentration were described in a previous paper [5] and, hence, are described here briefly. Fig. 1a shows temperature-dependent change in fluorescence spectra (λ_{exc} = 530 nm) of **P1** in water. The polymer shows distinctive fluorescence of the RD unit at 540–640 nm. As shown in Fig. 2 (circle), the fluorescence intensity (571 nm) is very weak at <25 °C and >40 °C, but is strong at 25–40 °C,

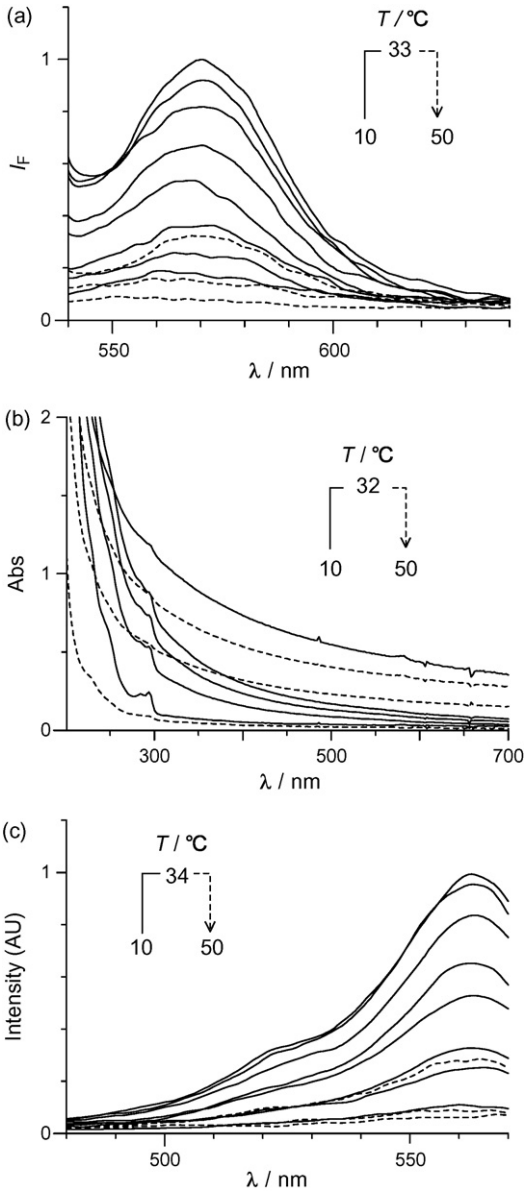

Fig. 1. Temperature-dependent change in (a) fluorescence (λ_{exc} = 530 nm), (b) absorption, and (c) excitation spectra (λ_{em} = 580 nm) of **P1** in water (pH 2.0) with 0.2 g L^{-1} concentration (containing 18.4 μmol L^{-1} RD unit). The fluorescence intensity (λ_{em} = 571 nm) of **P1** at 33 °C is set as 1. The measurements were done during heating sequence.

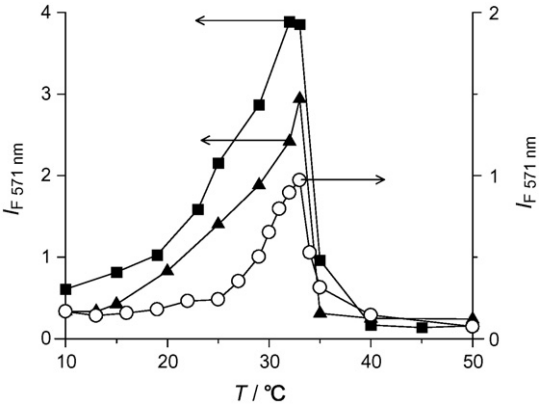

Fig. 2. Temperature-dependent change in fluorescence intensity (λ_{exc} = 530 nm; λ_{em} = 571 nm) of **P1** in water (pH 2.0) with concentrations of (square) 1.0 g L^{-1}, (triangle) 0.5 g L^{-1}, and (circle) 0.2 g L^{-1}, respectively. The detailed fluorescence spectra for 1.0 and 0.5 g L^{-1} are shown in Figs. S1 and S2, respectively.

showing an "*off–on–off*" intensity profile against the temperature window. The selective emission enhancement at 25–40 °C is due to the heat-induced structure change of the polymer from *coil* to *globule* (Scheme 3). At low temperature, the polymer exists as a polar coil state due to hydration of the polymer chain [14,15]. However, at >25 °C, dehydration of the polymer chain leads to polymer aggregation (globule state). As shown in Figs. 1b and 3a (circle),

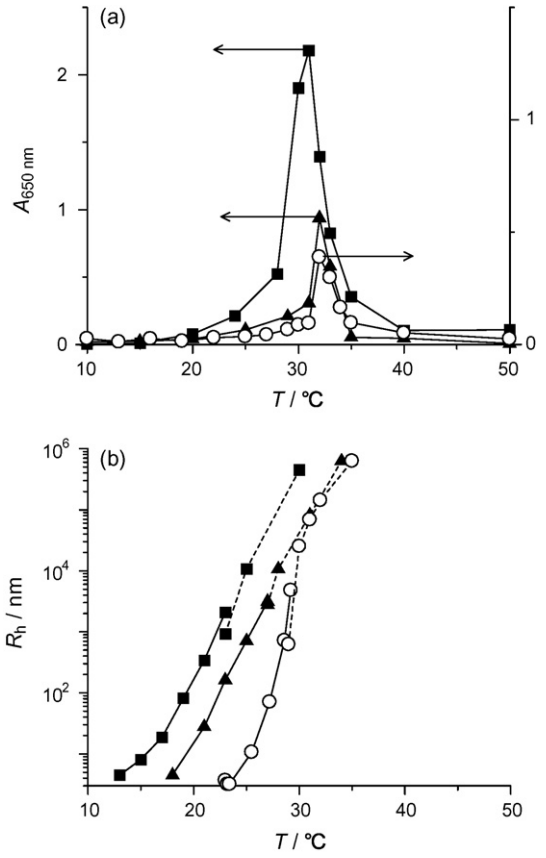

Fig. 3. Temperature-dependent change in (a) turbidity ($A_{650\ nm}$) and (b) hydrodynamic radius (R_h) of **P1** in water (pH 2.0) with concentration of (square) 1.0 g L^{-1}, (triangle) 0.5 g L^{-1}, and (circle) 0.2 g L^{-1}, respectively. The R_h data for solid and dotted lines were obtained by dynamic and static laser scattering measurements, respectively. The detailed R_h distribution data for these samples are summarized in Figs. S3, S4, and S5, respectively.

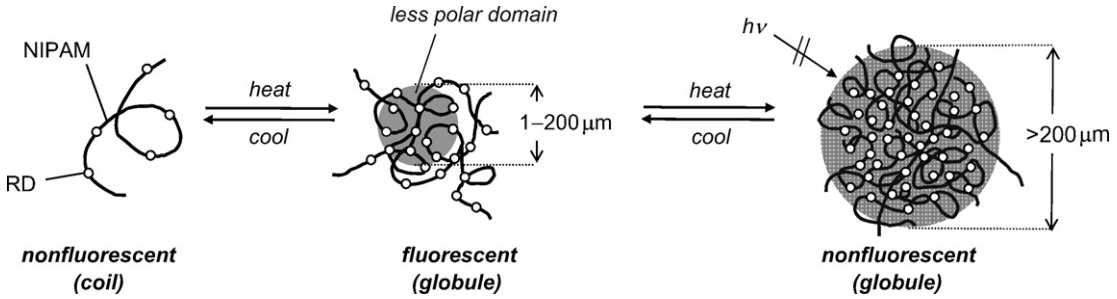

Scheme 3. Schematic representation of temperature-dependent fluorescence enhancement/quenching mechanism of RD-conjugated acrylamide polymer in water.

turbidity of the polymer solution ($A_{650\ nm}$) increases at >25 °C. In addition, as shown in Fig. 3b (circle), dynamic light scattering analysis detects the formation of polymer particle at >25 °C (detection limit: 3 nm), and the hydrodynamic radius (R_h) of the particles increases with a rise in temperature. The increases in the turbidity and particle size are consistent with the fluorescence intensity increase at >25 °C (Fig. 2, circle). In the globule state polymer, a less polar domain forms within the particle [14,15]. As described [6], quantum yield of the RD fluorescence increases with a decrease in the polarity of the medium. The less polar domain formation, therefore, leads to fluorescence enhancement at >25 °C (Fig. 2, circle). The less polar domain formation is confirmed by ^{1}H NMR analysis. Fig. 4a shows ^{1}H NMR spectra of **P1** dissolved in D_2O, and Fig. 4b shows the temperature-dependent change in the integrated proton intensity of the C*H* resonances of the polymer chain and the NIPAM unit. The proton intensity scarcely changes at low temperature, but decreases with a rise in temperature >25 °C, indicating that less polar domain indeed forms and the polarity decreases with a rise in temperature. The size of the polymer particle showing the highest fluorescence intensity (33 °C) is estimated to be 143 μm.

The decrease in the fluorescence intensity at >33 °C (Fig. 2, circle) is due to the strong polymer aggregation, leading to formation of huge polymer particles. As shown in Fig. 3b (circle), the size of the polymer particles becomes >200 μm at >33 °C. As shown in Fig. 3a (circle), at this temperature range, the solution turbidity decreases because the solution transparency increases by the huge polymer particle formation. The formed huge polymer particles suppress the incident light absorption by the RD unit within the particles, leading to fluorescence quenching at >33 °C (Fig. 2, circle). The above fluorescence enhancement/quenching of the **P1** polymer occurs reversibly regardless of the heating or cooling sequence. In addition, the polymer can be recovered simply by centrifugation at high temperature, and the recovered polymer shows the same fluorescence behavior as the virgin polymer [5].

3.2. Effect of polymer concentration

Effect of polymer concentration on the fluorescence property was studied with **P1** polymer. The square and triangle symbols in Fig. 2 show the change in fluorescence intensity of **P1** measured with 1.0 and 0.5 g L^{-1} concentrations, respectively. Both cases show "*off–on–off*" fluorescence intensity profile. With 0.2 g L^{-1} polymer (circle), fluorescence intensity increases at >25 °C. However, at higher concentrations, the increase starts at even lower temperature (<15 °C). This is because high polymer concentration leads to polymer aggregation even at lower temperature due to enhanced interpolymer association [7]. As shown in Fig. 3a (square and triangle), with 1.0 and 0.5 g L^{-1} polymer, the increase in the solution turbidity takes place at lower temperature as compared to the case with 0.2 g L^{-1} polymer (circle). This indicates that, at higher polymer concentration, polymer aggregation actually occurs at lower temperature. This is confirmed by the polymer particle size; as shown in Fig. 3b (square and triangle), at higher polymer concentration, the polymer particles form at lower temperature. These findings clearly indicate that higher polymer concentration enhances the polymer aggregation and the formation of less polar

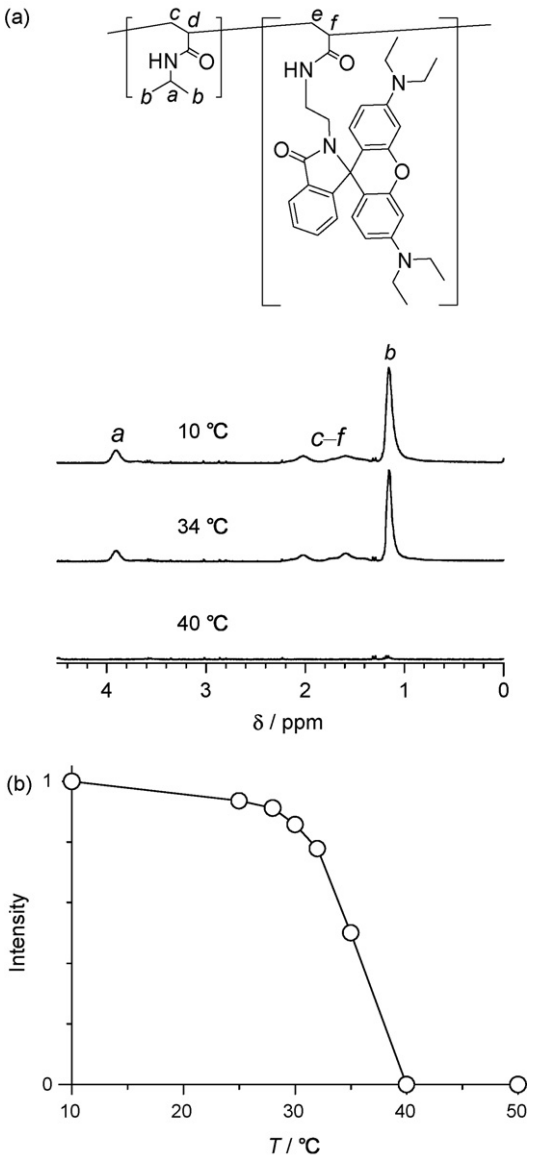

Fig. 4. (a) Temperature-dependent change in partial ^{1}H NMR spectra of **P1** measured in D_2O (pH 2.0). (b) Change in the integrated proton intensity of C*H* resonances of the polymer chain and NIPAM unit for **P1** as a function of temperature. The C*H* intensity at 10 °C is set as 1.

domain at lower temperature and, hence, results in fluorescence enhancement at lower temperature.

As shown in Fig. 3b (square and triangle), with 1.0 and 0.5 g L^{-1} polymer, the size of polymer particles become >200 μm at c.a. >33 °C, as is also the case with 0.2 g L^{-1} polymer. As shown in Fig. 3a, at this temperature range, the solution turbidity decreases accordingly. These indicate that, also at these concentrations, the huge polymer particle formation suppresses the incident light absorption by the RD unit within the particles, leading to fluorescence quenching at c.a. >33 °C (Fig. 2). The obtained fluorescence intensity–temperature profiles reveal that the use of higher concentration of the RD-conjugated acrylamide polymer makes the detectable (emissive) temperature range widen to lower temperature.

3.3. Effect of adding other acrylamide components

Effect of adding other acrylamide components (NNPAM and NIPMAM) to the polymer on the fluorescence properties was studied. As described [3a,c–e], aggregation of polyNNPAM and polyNIPMAM takes place at lower (ca. 19 °C) and higher temperature (ca. 46 °C) than that of polyNIPAM (ca. 31 °C). We synthesized two types of polymers, poly(NIPAM-*co*-NNPAM-*co*-RD) (**P2**) and poly(NIPAM-*co*-NIPMAM-*co*-RD) (**P3**), both containing similar amount of NNPAM or NIPMAM component to that of NIPAM. The properties of the respective **P2** and **P3** polymers are summarized in Table 1. Fig. 5 shows the temperature-dependent changes in fluorescence intensity (λ_{exc} = 530 nm; λ_{em} = 571 nm) of the respective polymers measured in water with concentration of 0.2 g L^{-1}. **P2** polymer shows fluorescence enhancement at 25–30 °C with a maximum intensity at 27 °C. In contrast, **P3** polymer shows enhancement at 40–55 °C with a maximum intensity at 46 °C. These data clearly reveal that the addition of NNPAM and NIPMAM components within the polymer changes the detectable (emissive) temperature region to either lower or higher temperature.

Fig. 6a shows change in turbidity of the solution containing the respective polymers. The turbidity increase of the **P2** polymer solution occurs at >20 °C. As shown in Fig. 6b, the polymer particle forms also at >20 °C. These occur at lower temperature than the case with **P1** polymer (>25 °C), and the data are consistent with the fluorescence intensity increase (Fig. 5). With **P3** polymer, the turbidity increase and the polymer particle formation occur at higher temperature (>35 °C), and the data are also consistent with the fluorescence intensity increase (Fig. 5). Fig. 6c shows temperature-dependent change in the integrated proton intensity of the C*H* resonances for the respective polymers measured by ^{1}H NMR. The intensity decrease of the **P2** and **P3** polymers agrees reasonably well with the increases in the solution turbidity (Fig. 6a), the particle size (Fig. 6b), and the fluorescence intensity (Fig. 5). These data clearly indicate that the addition of NNPAM or NIPMAM leads to a shift of the temperature for polymer aggregation and less polar domain formation.

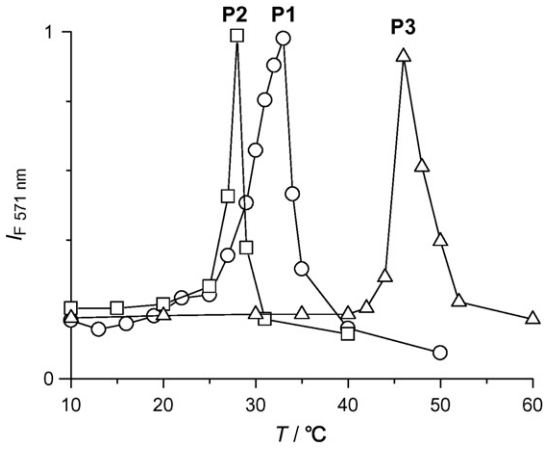

Fig. 5. Temperature-dependent change in fluorescence intensity (λ_{exc} = 530 nm; λ_{em} = 571 nm) of **P1**, **P2**, and **P3** polymers measured in water (pH 2.0) with concentration of 0.2 g L^{-1}. The detailed fluorescence, absorption, and excitation spectra of **P2** and **P3** polymers are summarized in Figs. S6 and S7, respectively.

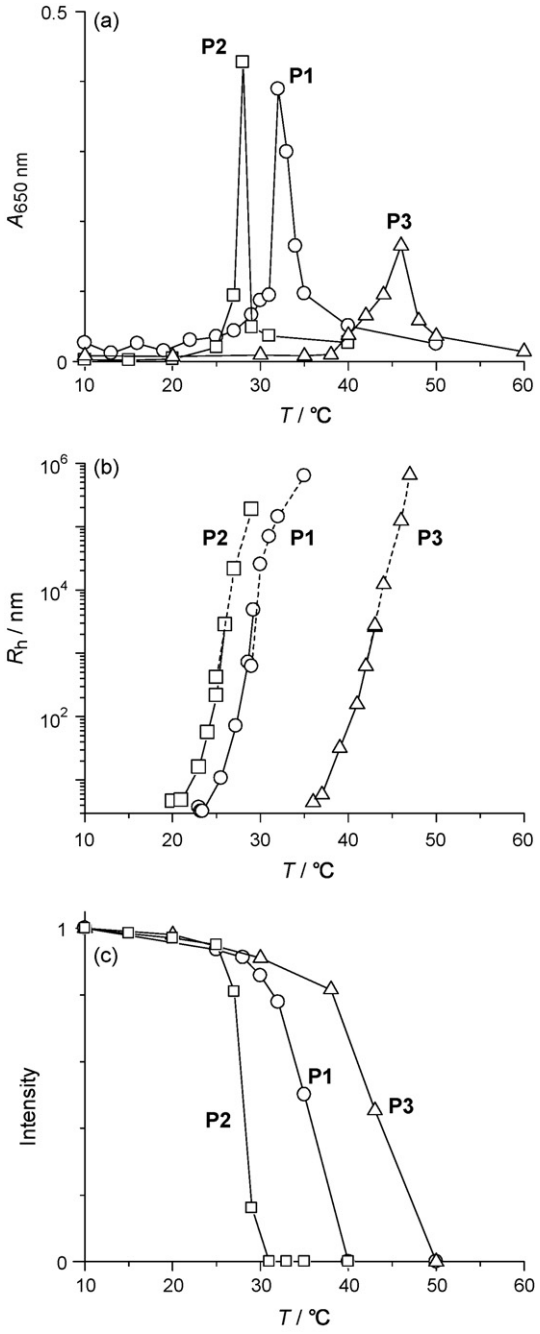

Fig. 6. Temperature-dependent change in (a) turbidity ($A_{650\ nm}$), (b) hydrodynamic radius (R_h), and (c) integrated proton intensity of C*H* resonance of **P1**, **P2**, and **P3** polymers in water (pH 2.0) with concentration of 0.2 g L^{-1}. The R_h data for solid and dotted lines were obtained by dynamic and static laser scattering methods, respectively. The detailed R_h distribution data for **P2** and **P3** polymers are summarized in Figs. S8 and S9, respectively. The change in ^{1}H NMR spectra for **P2** and **P3** polymers are summarized in Figs. S10 and S11, respectively.

As shown in Fig. 6b, the size of the polymer particle becomes >200 μm at >33 °C (**P1**), >27 °C (**P2**), and >46 °C (**P3**). At these temperatures, both solution turbidity (Fig. 6a) and fluorescence intensity (Fig. 5) decrease simultaneously. These data suggest that, for both **P2** and **P3** polymers, the incident light absorption by the RD units are suppressed by the huge polymer particles, resulting in fluorescence quenching at higher temperature. The obtained fluorescence intensity–temperature profiles (Fig. 5) clearly reveal that the addition of other acrylamide components to the polymer enables the detectable (emissive) temperature region to shift to either lower or higher temperature.

4. Conclusion

Fluorescence behaviors of RD-conjugated NIPAM polymers, exhibiting selective emission enhancement at specific temperature ranges, have been studied in water. Effects of polymer concentration and addition of other acrylamide components to the polymer have been investigated, with the following results:

(1) Poly(NIPAM-*co*-RD) dissolved in water with 0.2 g L^{-1} concentration shows selective fluorescence enhancement at 25–40 °C. At higher polymer concentration, the emissive temperature range is widened to lower temperature; use of 1.0 and 0.5 g L^{-1} concentration shows fluorescence enhancement at 10–40 and 15–40 °C, respectively. This is because higher polymer concentration enhances the polymer aggregation, leading to less polar domain formation to start at lower temperature.
(2) Addition of other acrylamide components to poly(NIPAM-*co*-RD) enables the emissive temperature region to shift to either lower or higher temperature; poly(NIPAM-*co*-NNPAM-co-RD) and poly(NIPAM-*co*-NIPMAM-*co*-RD) show selective fluorescence enhancement at 25–30 °C and 40–55 °C, respectively. This is because the addition of NNPAM or NIPMAM monomer leads to a shift of aggregation temperature of the polymer.

Acknowledgments

This work was partly supported by the Grant-in-Aids for Scientific Research (no. 19760536) from the Ministry of Education, Culture, Sports, Science and Technology, Japan (MEXT). We thank the Division of Chemical Engineering for the Lend-Lease Laboratory System.

Appendix A. Supplementary data

Supplementary data associated with this article can be found, in the online version, at doi:10.1016/j.jphotochem.2008.08.020.

References

[1] For books and reviews:
(a) F. Otón, A. Espinosa, A. Tárraga, C.R. de Arellano, P. Molina, Chem. Eur. J. 13 (2007) 5742–5752;
(b) S.W. Thomas III, G.D. Joly, T.M. Swager, Chem. Rev. 107 (2007) 1339–1386;
(c) M. Burnworth, S.J. Rowan, C. Weder, Chem. Eur. J. 13 (2007) 7828–7836;
(d) J.S. Kim, D.T. Quang, Chem. Rev. 107 (2007) 3780–3799;
(e) F.M. Raymo, M. Tomasulo, Chem. Soc. Rev. 34 (2005) 327–336;
(f) A.P. de Silva, D.B. Fox, T.S. Moody, S.M. Weir, Trends Biotechnol. 19 (2001) 29–34;
(g) L. Fabbrizzi, M. Licchelli, L. Parodi, A. Poggi, A. Taglietti, J. Fluoresc. 8 (1998) 263–271;
(h) A.P. de Silva, H.Q.N. Gunaratne, T. Gunnlaugsson, A.J.M. Huxley, C.P. McCoy, J.T. Rademacher, T.E. Rice, Chem. Rev. 97 (1997) 1515–1566.
[2] Molecule-based sensors:
(a) G.A. Baker, S.N. Baker, T.M. McCleskey, Chem. Commun. (2003) 2932–2933;
(b) J.M. Lupton, Appl. Phys. Lett. 81 (2002) 2478–2480;
(c) C. Baleizão, S. Nagl, S.M. Borisov, M. Schäferling, O.S. Wolfbeis, M.N. Berberan-Santos, Chem. Eur. J. 13 (2007) 3643–3651;
(d) B. Dong, D.P. Liu, X.J. Wang, T. Yang, S.M. Miao, C.R. Li, Appl. Phys. Lett. 90 (18117) (2007) 1–3;
(e) M. Engeser, L. Fabbrizzi, M. Licchelli, D. Sacchi, Chem. Commun. (1999) 1191–1192.
[3] Polymer-based sensors:
(a) S. Uchiyama, Y. Matsumura, A.P. de Silva, Anal. Chem. 75 (2003) 5926–5935;
(b) S. Uchiyama, N. Kawai, A.P. de Silva, K. Iwai, J. Am. Chem. Soc. 126 (2004) 3032–3033;
(c) S. Uchiyama, Y. Matsumura, A.P. de Silva, K. Iwai, Anal. Chem. 76 (2004) 1793–1798;
(d) K. Iwai, Y. Matsumura, S. Uchiyama, A.P. de Silva, J. Mater. Chem. 15 (2005) 2796–2800;
(e) C. Gota, S. Uchiyama, T. Ohwada, Analyst 132 (2007) 121–126;
(f) F.M. Winnik, Macromolecules 23 (1990) 233–242;
(g) Y.S. Avlasevich, T.A. Chevtchouk, V.N. Knyukshto, O.G. Kulinkovich, K.N. Solovyov, J. Porphyrins Phthalocyanines 4 (2000) 579–587;
(h) C.-C. Yang, Y. Tian, C.-Y. Chen, A.K.-Y. Jen, W.-C. Chen, Macromol. Rapid Commun. 28 (2007) 894–899;
(i) Y. Shiraishi, R. Miyamoto, T. Hirai, Langmuir 24 (2008) 4273–4279.
[4] (a) J. Lou, T.A. Hatton, P.E. Laibinis, Anal. Chem. 69 (1997) 1262–1264;
(b) Z. Wang, D. Zhang, D. Zhu, Tetrahedron Lett. 46 (2005) 4609–4612;
(c) Q. Zeng, Z. Li, Y. Dong, C. Di, A. Qin, Y. Hong, L. Ji, Z. Zhu, C.K.W. Jim, G. Yu, Q. Li, Z. Li, Y. Liu, J. Qin, B.Z. Tang, Chem. Commun. (2007) 70–72;
(d) D. Ross, M. Gaitan, L.E. Locascio, Anal. Chem. 73 (2001) 4117–4123;
(e) M.E. Köse, B.F. Carroll, K.S. Schanze, Langmuir 21 (2005) 9121–9129;
(f) G. Kwak, S. Fukao, M. Fujiki, T. Sakaguchi, T. Masuda, Chem. Mater. 18 (2006) 2081–2085;
(g) X. Guan, X. Liu, Z. Su, J. Appl. Polym. Sci. 104 (2007) 3960–3966;
(h) K.F. Schrum, A.M. Williams, S.A. Haerther, D. Ben-Amotz, Anal. Chem. 66 (1994) 2788–2790;
(i) S. Wang, S. Westcott, W. Chen, J. Phys Chem. B 106 (2002) 11203–11209;
(j) T. Corrales, C. Abrusci, C. Peinado, F. Catalina, Macromolecules 37 (2004) 6596–6605.
[5] Y. Shiraishi, R. Miyamoto, X. Zhang, T. Hirai, Org. Lett. 9 (2007) 3921–3924.
[6] (a) M.J. Snare, F.E. Treloar, K.P. Ghiggino, P.J. Thistlethwaite, J. Photochem. 18 (1982) 335–346;
(b) T.-L. Chang, H.C. Cheung, J. Phys. Chem. 96 (1992) 4874–4878;
(c) R.S. Moog, M.D. Ediger, S.G. Boxer, M.D. Fayer, J. Phys. Chem. 86 (1982) 4694–4700.
[7] (a) W. Zhang, L. Shi, K. Wu, Y. An, Macromolecules 38 (2005) 5743–5747;
(b) B. Işık, Y. Günay, Colloid Polym. Sci. 282 (2004) 693–698.
[8] H. Ringsdorf, J. Venzmer, F.M. Winnik, Macromolecules 24 (1991) 1678–1686.
[9] Y. Xiang, A. Tong, Org. Lett. 8 (2006) 1549–1552.
[10] H. Ringsdorf, J. Simons, F.M. Winnik, Macromolecules 25 (1992) 5353–5361.
[11] (a) Y. Shiraishi, C. Ichimura, T. Hirai, Tetrahedron Lett. 48 (2007) 7769–7773;
(b) Y. Shiraishi, H. Maehara, K. Ishizumi, T. Hirai, Org. Lett. 9 (2007) 3125–3128;
(c) Y. Shiraishi, Y. Tokitoh, T. Hirai, Chem. Commun. (2005) 5316–5318.
[12] (a) Y. Shiraishi, Y. Tokitoh, T. Hirai, Org. Lett. 8 (2006) 3841–3844;
(b) Y. Shiraishi, Y. Tokitoh, G. Nishimura, T. Hirai, Org. Lett. 7 (2005) 2611–2614;
(c) G. Nishimura, Y. Shiraishi, T. Hirai, Chem. Commun. (2005) 5313–5315;
(d) G. Nishimura, M. Maehara, Y. Shiraishi, T. Hirai, Chem. Eur. J. 14 (2008) 259–271.
[13] Y. Shiraishi, R. Miyamoto, T. Hirai, Tetrahedron Lett. 48 (2007) 6660–6664.
[14] (a) H. Koizumi, Y. Shiraishi, S. Tojo, M. Fujitsuka, T. Majima, T. Hirai, J. Am. Chem. Soc. 128 (2006) 8751–8753;
(b) H. Koizumi, Y. Kimata, Y. Shiraishi, T. Hirai, Chem. Commun. (2007) 1846–1848.
[15] (a) Y. Ono, T. Shikata, J. Am. Chem. Soc. 128 (2006) 10030–10031;
(b) N. Ishida, S. Biggs, Langmuir 23 (2007) 11083–11088;
(c) T. Miyamae, H. Akiyama, M. Yoshida, N. Tamaoki, Macromolecules 40 (2007) 4601–4606;
(d) T. Mori, M. Maeda, Langmuir 20 (2004) 313–319.